Min-Jay Chung and Sheng-Yang Wang*

Mechanical properties of oriented bamboo scrimber boards made of *Phyllostachys pubescens* (moso bamboo) from Taiwan and China as a function of density

https://doi.org/10.1515/hf-2017-0084
Received May 18, 2017; accepted September 11, 2017; previously published online October 17, 2017

Abstract: The properties of oriented bamboo scrimber boards (OBSB) have been investigated at three density levels (0.8, 0.9, and 1.0 g cm^3), while the boards were made from moso bamboo (*Phyllostachys pubescens*) grown in Taiwan (T-OBSB) and China (C-OBSB). A non-destructive technique (NDT), ultrasonic-wave velocity (V_u) measurements were applied and the dynamic modulus of elasticity (MOE_{dyn}) was calculated. Moreover, static modulus of elasticity (MOE), modulus of rupture (MOR), profile density distribution, internal bond strength (IB), springback (SB), and dimensional stability were determined based on traditional methods. Positive linear relationships between density and V_u, MOE_{dyn}, MOE and MOR were observed, no matter if the measurements were done parallel (//) or perpendicular (⊥) to the fiber direction of the OBSBs. Moreover, $V_{u(//)}$, $MOE_{dyn,u(//)}$, $MOE_{(//)}$, and $MOR_{(//)}$ were higher than $V_{u(\perp)}$, $MOE_{dyn,u(\perp)}$, $MOE_{(\perp)}$ and $MOR_{(\perp)}$. C-OBSB had slightly lower $V_{u(//)}$, $V_{u(\perp)}$, $MOE_{dyn,u(//)}$ and $DMOE_{u(\perp)}$ values than T-OBSB. T-OBSB had higher $MOE_{(//)}$, $MOE_{(\perp)}$ and $MOR_{(//)}$ than C-OBSB, but less $MOR_{(\perp)}$. The profile density distribution of high-density T-OBSB showed singnificant data scattering. The profile density distribution of C-OBSB was homogeneous at all density levels. IB and SB data are directly proportional to density, but water absorption, thickness swelling and volumetric swelling are inversely proportional to density. T-OBSB has better bonding and strength properties, and dimensional stability than C-OBSB.

Keywords: dimensional stability, dynamic modulus of elasticity (MOE_{dyn}), mechanical property, modulus of rupture (MOR), moso bamboo, oriented bamboo scrimber board (OBSB), *Phyllostachys pubescens*, physical properties, spring back behavior (SB), static modulus of elasticity (MOE), water absorption (WA%)

***Corresponding author: Sheng-Yang Wang,** Department of Forestry, National Chung-Hsing University, Taichung, 402, Taiwan; and Agricultural Biotechnology Research Center, Academia Sinica, Taipei, Taiwan, Phone: + 886-4-22840345, ext 138, e-mail: taiwanfir@dragon.nchu.edu.tw
Min-Jay Chung: Experimental Forest, National Taiwan University, Taipei, Taiwan; and Department of Forestry, National Chung-Hsing University, Taichung, Taiwan

Introduction

Bamboo is a renewable natural resource, which is widely used due to its excellent properties, such as rapid growth, good flexibility and its short production period. Moreover, bamboo has a high CO_2 sequestration efficiency. A variety of bamboo culm utilizations are attracting increasing global attention (Khalil et al. 2012). Among others, moso bamboos (*Phyllostachys pubescence* and *Phylostachys* sp.) have very interesting mechanical, anatomical and chemical properties. This is the reason why moso bamboo is the focus of intensive basic and applied research concerning their physical and chemical properties (Qu et al. 2012; Wen et al. 2013; Liu et al. 2015, 2016; Li et al. 2015, 2017; Wang et al. 2016; Huang et al. 2017). Both bamboo culm and wood timber possess similar mechanical and strength properties. Engineered bamboo products sometimes increase the properties of corresponding timber products (Sharma et al. 2015a). Khalil et al. (2012) applied bamboo fiber for reinforcement of composites. Obataya et al. (2007) developed a fiber-foam composite structures based on moso bamboo (*P. pubescens*). Composed materials were also developed, such as laminated bamboo board (LBB) (Lee et al. 1998; Lee and Liu 2003; Okubo et al. 2004; Obataya et al. 2007; Sulastiningsih and Nurwati 2009; Lee et al. 2012; Verma and Chariar 2012). LBB is widely used, but in this material some of the unique properties of bamboo are lost and the process is expensive. In a similar fashion as in the case of oriented strand board (OSB) from wood, the oriented bamboo scrimber board (OBSB) has also attracted popularity and research interest (Wang 1989; Yu and Yu 2013; Yu et al. 2015; Sharma et al. 2015a,b). The slenderness ratio of OBSB is higher than that of LBB and it has better mechanical properties (Sharma et al. 2005a,b). The raw material utilization rate of OBSB is better than that of LBB (Yu et al. 2005) and its production is less expensive.

Earlier, composites made of bamboo had low bonding strength and rough structure (Wang 1989; Nugroho

Brought to you by | National Chung Hsing University
Authenticated
Download Date | 6/16/18 5:13 AM

and Ando 2001). This situation has improved a lot due to advances in manufacturing technology, as regards equipment, adhesives and the introduction of hot pressing technology. This is the reason why new OBSB products have a better surface texture, greater hardness, and better longitudinal strength (Yu and Yu 2013). Meanwhile, 600 000 m^3 of OBSB is produced in China (Yu and Yu 2013), these are used for flooring, furniture, construction and civil engineering.

The key properties of bamboo are high strength, density, dynamic modulus of elasticity (MOE_{dyn}), static modulus of elasticity (MOE) and modulus of rupture (MOR) (Mishiro 1996). Ross (2015) demonstrated a good correlation between the MOE_{dyn} and MOE of timber. Lin et al. (2006) and Lee et al. (2012) evaluated the quality of LBB made of moso bamboo by non-destructive techniques (NDTs) and found good positive relationships between MOE_{dyn} and MOE, while the relationship between MOE_{dyn} and MOR was excellent with R^2 of 0.92. Moreover, the NDT methods based on ultrasonic waves in the quoted studies proved to be effective in assessing the mechanical strength of LBBs.

In the present study, an ultrasonic NDT and other traditional characterization methods were conducted to evaluate the mechanical properties of OBSB made from moso bamboo grown in China and Taiwan. Among others, MOE, MOR, the profile density distribution, internal bond strength (IB), springback (SB), and dimensional stability of the OBSBs are assessed. In focus was the question whether the OBSBs made of moso bamboo grown in different regions have deviating mechanical behavior.

Materials and methods

Three-year-old moso bamboo (*Phyllostachys pubescens* Mazel) culms were collected from the Experimental Forest of National Taiwan University (Nan-Tou County, Taiwan) and Lin'an County (Zhejiang Province, China) in October 2015. The culms were cut into dimensions of 450 mm (l) × 20 mm (t) × 5 mm (r) and then stored at 4°C without exposure to light. Before use, culms were pre-treated with 0.5% water-based surfactant and 2% KOH at 100°C for 30 min and then oven-dried at 80°C.

Figure 1 illustrates the manufacturing process of OBSB specimens. Briefly, the bamboo culms were peeled and extruded into thin strips of 450 mm × 1–2 mm (length × width) by mechanical processing. The strips were dried at 80°C for 12 h and then placed in an iron frame of 450 × 450 × 12 mm (length × width × thickness) to form a scrimber board OBSB. A water-soluble urea formaldehyde resin (UF; Wood Glue Industrial, Tainan, Taiwan) with a solid content of 63.6% was applied (10% based on the raw material). The adhesive strips were hot-pressed under curing for 12 min at 120°C and the pressure used during hot-pressing was set to 100 kg cm^{-2}, followed by a cooling period of 10 min. All specimens were conditioned in a controlled environment (20°C, RH 65%) for 2 weeks before testing. Table 1 summarizes the codes and characteristics for the six types of OBSB specimens.

Characterization and analysis

The ultrasonic-wave velocity and the MOE_{dyn} were measured by means of a portable ultrasonic NDT device (Sylvatest Duo, Saint Sulpice, Switzerland) at 22 kHz. Specimens were placed between the transmitting and receiving transducers, and the transmission time was recorded. In Eqs. (1) and (2) used for calculation of MOE_{dyn}: V_u is the longitudinal ultrasonic – wave velocity of the specimen, t is the transmission time, L is the distance between the two transducers, T is the propagation time of pulse from transmitting transducer to receiving transducer and ρ is the density based on the mass-to-volume ratio of the specimen.

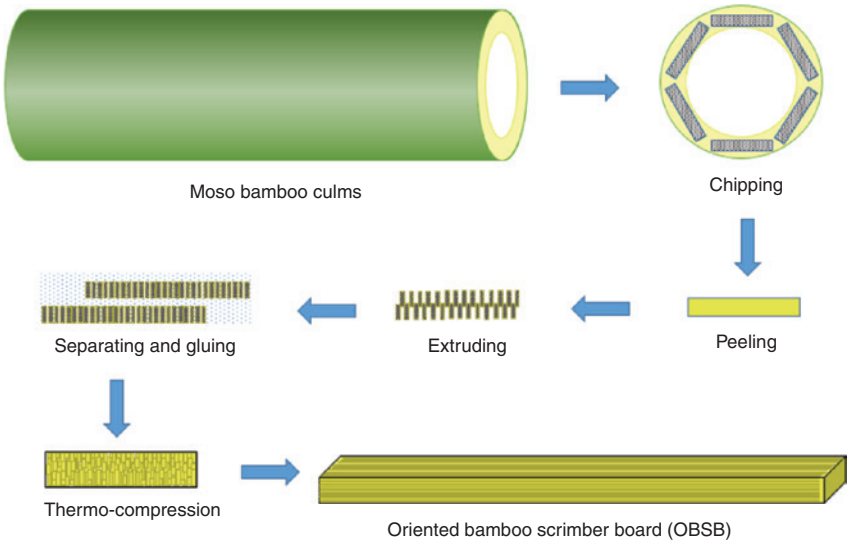

Figure 1: Manufacturing process of OBSB.

Brought to you by | National Chung Hsing University
Authenticated
Download Date | 6/16/18 5:13 AM

Table 1: Codes and characteristics of OBSB specimens. In all cases three boards were investigated with nine replicates.

Origin	Target density (g cm^{-3})	Code
Taiwan	0.8	T-OBSB$_{0.8}$
	0.9	T-OBSB$_{0.9}$
	1.0	T-OBSB$_{1.0}$
China	0.8	C-OBSB$_{0.8}$
	0.9	C-OBSB$_{0.9}$
	1.0	C-OBSB$_{1.0}$

$$V_u = L/t \tag{1}$$

$$\mathrm{MOE}_{\mathrm{dyn},u} = V_u^2 \times \rho \tag{2}$$

The mechanical strength of OBSB specimens were examined according to the American Society Testing and Materials (ASTM) method standard D-1037. The static bending test was conducted on a Shimadzu UH-10A (Tokyo, Japan) universal-type testing machine by the center-loading method for specimens. A concentrated bending load was applied at the center of the sample with a span 15 times larger than the sample thickness. Both MOE and MOR were calculated from load-deflection curves according to Eqs. (3) and (4), where $P_{\max}$ is the maximum load, P_p is the load at the proportional limit, δ is the deflection corresponding to P_p, b is the width of the specimen, h is the thickness of the specimen and L is the span.

$$\mathrm{MOR\ (MPa)} = 3P_{\max}L/2bh^2 \tag{3}$$

$$\mathrm{MOE\ (GPa)} = P_pL^3/4\delta bh^3 \tag{4}$$

Figure 2 shows the schematic view of the OBSB specimen for profile density distribution analysis. The specimens were 50 mm × 50 mm × 12 mm (l × width × thickness). All the specimens were divided in half, with each half representing three OBSB layers. The dimensions of each OBSB layer were 50 mm × 50 mm × 2 mm (l × width × thickness). The density of each layer was calculated based on its weight and volume measured after each grinding using a sand mill.

The tensile strength perpendicular (⊥) to the surface was determined with nine square conditioned samples of 50 mm × 50 mm from each panel according to ASTM standard D-1037-96. The rupture load (P) was determined, and internal bond strength (IB) strength was calculated Eq. (5), where b is the width of the specimen, and L is the length of the sample.

$$\mathrm{IB\ (N\ mm^{-2})} = P/(b \times L) \tag{5}$$

$$\mathrm{SB\ (\%)} = 100(S_a - 12)/12 \tag{6}$$

Twelve millimeter thick specimens were placed in a controlled environment with 65% relative humidity (RH) for 2 weeks. The percentage of springback (SB) was calculated by Eq. (6), where S_a is the thickness after being placed in the controlled environment.

Dimensional stability of the OBSB specimens was tested according to ASTM standard D-1037 to determine volumetric swelling (S), thickness swelling (TS) and water absorption (WA). Initial thickness at the middle of the test specimen was first measured with a micrometer. Then all test samples were placed in parallel 30 mm under water and soaked for 2 and 24 h before the thickness was measured again. The S, TS and WA were determined by Eqs. (7–9), where the V_w is the volume in saturated state, V_o is the volume in oven-dried state, T_w is the thickness of saturated state, and T_o is the thickness of oven-dried state, W_w is the weight of saturated state, and W_o is the weight of the oven-dried state.

$$\mathrm{S\ (\%)} = 100\ (V_w - V_0)/V_0 \tag{7}$$

$$\mathrm{TS\ (\%)} = 100\ (T_w - T_0)/T_0 \tag{8}$$

$$\mathrm{WA\ (\%)} = 100\ (W_w - W_0)/W_0 \tag{9}$$

Data are presented as the mean of nine replicates with standard deviation (SD presented in parenthesis). The differences between the experimental specimens were checked by a Tukey's test and analysis of variance (ANOVA) in case of a significant difference. Numbers followed by different letters (a–e) are statistically different at the probability level of $P < 0.05$ according to Tukey's test and ANOVA. All analyses were performed by the software Statistical Analysis System 8.0 (SAS Institute Inc., Cary, NC, USA).

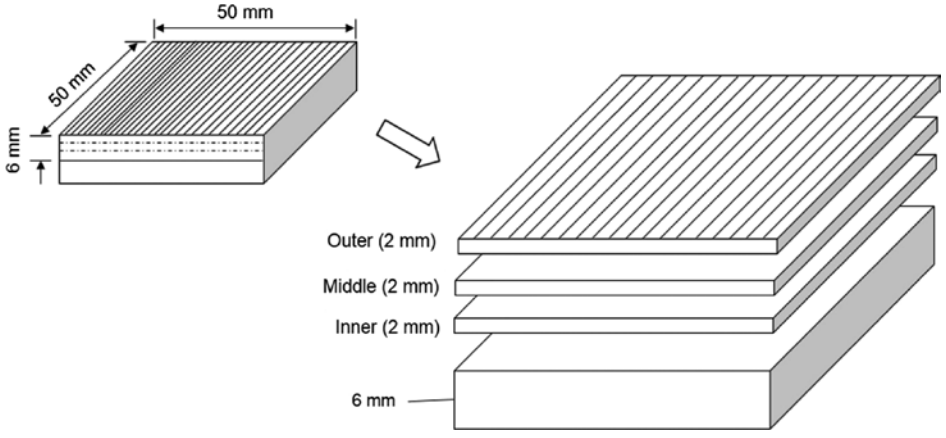

Figure 2: Schematic view for analysis of profile density.

Brought to you by | National Chung Hsing University
Authenticated
Download Date | 6/16/18 5:13 AM

Results and discussion

Ultrasonic-based dynamic properties

As shown in Table 2, the ultrasonic-wave velocity parallel to the fiber direction, $V_{u(//)}$, of T-OBSB specimens with increasing densities (0.8, 0.9, and 1.0 g cm^{-3}) were 4376, 4387, and 4410 ms^{-1}, respectively, i.e. there is a positive linear relationship. The corresponding data for C-OBSB are for the same densities 4043, 4133, and 4164 ms^{-1}, respectively. Thus C-OBSB have slightly lower $V_{u(//)}$ data than T-OBSB. Our results showed the C-OBSB (China bamboo) have slightly lower $V_{u(//)}$ data than T-OBSB (Taiwan bamboo). This data may be related to the results Oliveira et al. (2002), who found that chemical composition and microstructural characteristics are the most important factors influencing the $V_{u(//)}$ data. In the longitudinal direction, there is a greater continuity of cellulose crystalline regions, which are more influential. Thus, the $V_{u(//)}$ ultrasonic-wave velocity is greater than in other directions. Chung and Wang (2017) pointed out that moso bamboo from Taiwan had higher content of holocellulose (68.1%) and α-cellulose (47.9%) than that collected from moso bamboo in China (hollocellulose: 66.9% and cellulose: 43.8%). This could partially explain the $V_{u(//)}$ differences. Mishiro (1996) reported about similar correlations measured in both t- and r-directions of wood. Lee et al. (2012) demonstrated that $V_{u(//)}$ data of LBB flooring range from 4016 and 4174 ms^{-1}.

The $V_{u(\perp)}$ data (perpendicular to the fiber direction) are 1301, 1536, and 1623 ms^{-1} for T-OBSBs with increasing densities and 1304, 1506, and 1532 ms^{-1} for C-OBSB boards. A positive linear relationship between the data is obvious. Lee et al. (2012) obtained $V_{u(\perp)}$ of 1710 ms^{-1} for LLB flooring.

Moreover, $V_{u(\perp)}$ data are essentially lower than those of $V_{u(//)}$, which can be expected because of the orthotropic character of OBSBs, i.e. the small gaps between the fine strips in the transversal direction slow down the sound velocity. As is visible in Figure 3, the cross section of T-OBSB$_{0.8}$ has a high porosity, and the number of pores is decreasing with increasing densities. Wang et al. (2008) evaluated conifer woods (*Taiwania cryptomerioides*, *C. japonica*, *Pseudotsuga menziesii* and *Pinus* spp.) by NDT and found a positive correlation with the density.

As shown in Table 2, MOE$_{dyn,u(//)}$ of T-OBSB$_{0.8,0.9,1.0}$ were 15.7, 17.9 and 20.6 GPa, respectively. The data in terms of MOE$_{dyn,u(\perp)}$ are 1.4, 2.2 and 2.8 GPa, respectively; while C-OBSB$_{0.8,0.9,1.0}$ have MOE$_{dyn,u(//)}$ values of 13.2, 15.7 and 17.2 GPa and MOE$_{dyn,u(\perp)}$ of 1.4, 2.1 and 2.3 GPa, respectively.

Table 2: Average density, moisture content, ultrasonic-wave velocity, MOEdyn, MOE and MOR of six moso bamboo OBSB specimens.

			Dynamic data						
Samples	**ρ (g/cm^3)**	**MC (%)**	**$V_{u(//)}$ (ms^{-1})**	**$V_{u(\perp)}$ (ms^{-1})**	**MOE$_{u(//)}$ (GPa)**	**MOE$_{u(\perp)}$ (GPa)**	**MOE$_{(//)}$ (GPa)**	**MOE$_{(\perp)}$ (GPa)**	**MOR$_{(//)}$ (MPa)**	**MOR$_{(\perp)}$ (MPa)**
T-OBSB$_{0.8}$	0.82^{a} (0.02)	6.67^{a} (0.16)	4376^{c} (56)	1301^{a} (43)	15.70 (0.75)	1.39^{a} (0.08)	11.15^{c} (0.43)	0.89^{b} (0.12)	140.71^{c} (9.16)	4.82^{a} (0.73)
T-OBSB$_{0.9}$	0.93^{b} (0.03)	6.77^{a} (0.15)	4387^{c} (67)	1536^{c} (17)	17.90^{c} (0.82)	2.20^{b,c} (0.05)	12.89^{d} (0.61)	1.55^{d} (0.09)	172.88^{d} (5.86)	8.60^{b} (0.75)
T-OBSB$_{1.0}$	1.06^{c} (0.03)	6.37^{a} (0.25)	4410^{c} (52)	1623^{d} (35)	20.61^{d} (0.49)	2.79^{d} (0.13)	14.10^{e} (0.44)	2.09^{e} (0.09)	164.80^{d} (7.94)	10.60^{c,d} (1.63)
C-OBSB$_{0.8}$	0.81^{a} (0.02)	6.79^{a} (0.16)	4043^{a} (29)	1304^{a} (29)	13.24^{a} (0.40)	1.38^{a} (0.05)	7.45^{a} (0.45)	0.61^{a} (0.12)	107.13^{a} (8.25)	5.51^{a} (1.20)
C-OBSB$_{0.9}$	0.92^{b} (0.02)	6.82^{a} (0.20)	4133^{b} (31)	1506^{b} (20)	15.72^{b} (0.42)	2.09^{b} (0.07)	9.03^{b} (0.44)	1.25^{c} (0.05)	118.83^{a} (4.56)	9.93^{c} (1.01)
C-OBSB$_{1.0}$	0.99^{c} (0.02)	6.72^{a} (0.18)	4164^{b} (31)	1532^{c} (19)	17.17^{c} (0.45)	2.32^{c} (0.02)	9.77^{b} (0.30)	1.58^{d} (0.05)	125.31^{b} (6.34)	12.35^{c,d} (1.39)

Numbers followed by different letters (a–e) are statistically different at the probability level of $p < 0.05$ accoring to Tukey's test and ANOVA.

Brought to you by | National Chung Hsing University
Authenticated
Download Date | 6/16/18 5:13 AM

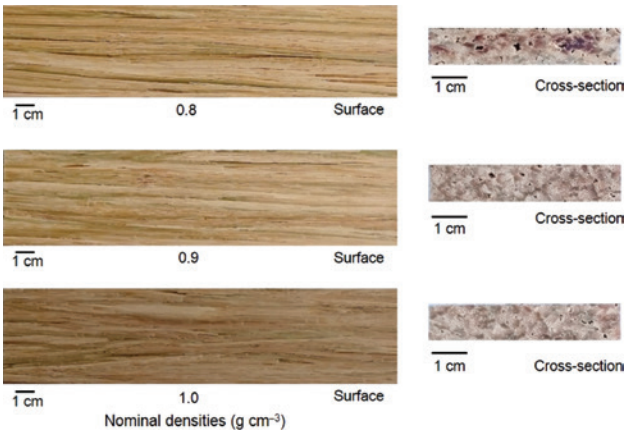

Figure 3: Morphology observation of T-OBSB of different densities.

Also these correlations are positive. $MOE_{dyn,u(//)}$ values are significantly higher than $MOE_{dyn,u(\perp)}$ and T-OBSB data are higher than those of C-OBSB. Lee et al. (2012), found $MOE_{dyn,u(//)}$ and $MOE_{dyn,u(\perp)}$ of LLB flooring of 10.4 and 1.9 GPa, respectively. The better data are due to the thermal compression in the manufacturing process leading to higher densities.

Mechanical properties

The $T\text{-}OBSB_{0.8,0.9,1.0}$ boards provided $MOE_{(//)}$ values of 11.1, 12.9 and 14.1 GPa, and $MOE_{(\perp)}$ 0.9, 1.5, and 2.1 GPa, respectively. These $MOE_{u(//)}$ data are for the samples C-OBSB are 7.4, 9.0 and 9.8 GPa and for $MOE_{(\perp)}$ 0.6, 1.2 and 1.6 GPa, respectively (Table 2). The $MOE_{(//)}$ values are significantly higher than $MOE_{(\perp)}$ but the correlation trends are similar; T-OBSB samples show higher $MOE_{(//)}$ and $MOE_{(\perp)}$ values than the C-OBSB samples.

T-OBSB samples have higher $MOE_{(//)}$ and $MOE_{(\perp)}$ values than the C-OBSB samples. From the mechanical properties of view, Chung and Wang (2017) demonstrated that 3-year-old moso bamboo culms collected from Taiwan had higher MOE values (10.7 GPa) than those from China (9.5 GPa) to the fiber direction. Chung and Wang (2017) reported that moso bamboo culms collected from Taiwan also had higher MOR values (158.9 MPa) than those from China (127.9 MPa). The most reasonable way to interpret these data is again using the higher cellulose content of Taiwan bamboo and this difference is transferred the OBSB boards. Wang et al. (2008) reported that MOE of *Taiwania cryptomerioides* and *Cryptomeria japonica* were 9.1 and 9.4 GPa, respectively; that is, the MOE of T-OBSB is higher than that of these two softwoods. The $MOE_{(//)}$ for LLB flooring is slightly lower (9.1 GPa) and the $MOE_{(\perp)}$ is higher (2.6 GPa) (Lee et al. 2012). The bonding strength between the bamboo strips in OBSB is lower than that between the lamina of LLB.

The positive correlation trends of MOR and MOE are similar in all configurations (Table 2). $MOR_{(//)}$ values are significantly higher than $MOR_{(\perp)}$. However, T-OBSB-$MOE_{(//)}$ is higher than C-OBSB-$MOE_{(//)}$, and C-OBSB-$MOE_{(\perp)}$ is higher than T-OBSB-$MOE_{(\perp)}$. Chung and Wang (2017) described that 3-year-old moso bamboo culms collected from Taiwan had higher MOR value (158.9 MPa) than that from China (127.9 MPa). $MOR_{(//)}$ data first increased with density, reached a plateau at 0.9 g cm^{-3} and then declined at higher densities. $MOR_{(//)}$ data of LLB flooring are much lower (95.6 MPa). In contrast, the $MOR_{(\perp)}$ data of LLB flooring is much higher (15.8 MPa) (Lee et al. 2012). This is due to a lower transverse strength of OBSBs as a result of poorer bonding among bamboo strips.

Profile density distribution (PDD) of wood composite is an important index for quality judgement. As a rule, the high-temperature compression leads to a higher density of the outer layers compared to that of the middle layers in wood composites (Winistorfer et al. 1995). Figure 4 presents

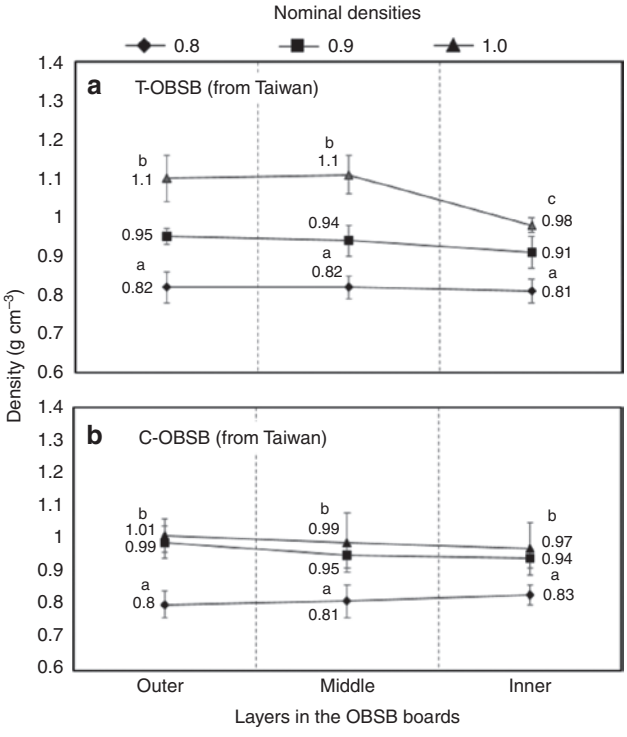

Figure 4: Profile densities of OBSBs made of moso bamboo: T-OBSB (a) and C-OBSB (b).
Numbers followed by different letters (a–c) are statistically different at the probability level of $P < 0.05$ according to Tukey's test and ANOVA.

Brought to you by | National Chung Hsing University
Authenticated
Download Date | 6/16/18 5:13 AM

corresponding data of OBSB. There are significant variations in profile density concerning the outer, middle and inner layers between T-OBSB$_{0.8}$ and T-OBSB$_{0.9}$ ($P < 0.05$). In contrast, the profile density differences are significant for T-OBSB$_{1.0}$ with 1.1, 1.1, and 0.98 g cm^{-3} for the outer, middle and inner layers, respectively ($P > 0.05$). T-OBSB with higher density show larger variations in PDD than those with lower densities (T-OBSB$_{0.8}$ and T-OBSB$_{0.9}$). In case of C-OBSB, the changes in PDD were insignificant depending of density ($P < 0.05$), i.e. the PDDs are relatively uniform.

Figure 5a illustrates the IB variations vs. OBSB densities revealing positive linear relationships. Lin and Huang (2001) found in the case of particle boards, higher IB with higher densities. The hot pressing process produces a higher densification of the particle mat, which in turn enhances the gluing quality and the IB.

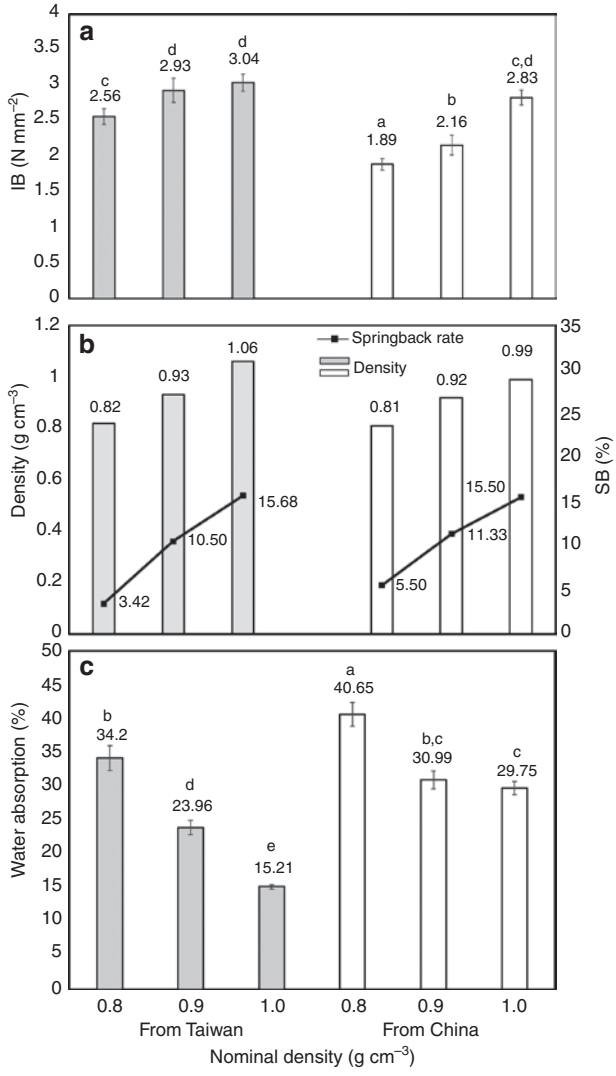

Figure 5: Properties of OBSB boards made of moso bamboo from Taiwan and China as a function of the densities.
Numbers followed by different letters (a–d) are statistically different at the probability level of $P < 0.05$ according to Tukey's test and ANOVA. (a) Internal bond strength; (b) spring back property (% SB); (c) water absorption (% WA).

The IB of all six OBSB specimens meets the requirements of CNS 2215 24-10 standards in terms of surface particle board (0.3 N mm^{-2}) and EN 312 Europe cohesion strength (0.4 N mm^{-2}). T-OBSB has a higher IB than C-OBSB. All differences in IB are significant ($P > 0.05$). A possible reason for this could be differences in the chemical composition of the bamboo culms. Chung and Wang (2017) reported that moso bamboo from China contains more alcohol-benzene extractives (9.8%) than that from Taiwan (8.8%). Hon (2001) stated that all types of extractives (waxes, fats, resins, rubber and water-soluble substances) can affect gluing, the coating process, dimensional stability and durability of lignocellulosic materials. Cellulose as the main constituent of bamboo culms has the highest effects on the mechanical properties of bamboo-made composites.

Dimensional stability

There are positive linear relationships between springback (SB) rate and density (Figure 5b) for both sample groups. In the case of lower densities, the vessel and cell lumens are less affected but after hot pressing the higher densities affect the SB data more directly (Tabarsa and Chui 1997). Lee et al. (1996) described that the amount of adhesives influences the MOE MOR, IB and TS of bamboo strandboards, but not the SB, linear expansion or nail withdrawal resistance.

Figure 5c presents the water absorption percentages (WA%), which show inverse relationship to density with a significant statistical difference ($P > 0.05$). C-OBSB has higher WA% than T-OBSB and its WA% reduction is also smaller. Due to the abundant parenchyma cells and vessels the bamboo tissue is porous (Figure 3), but the hot pressing during OBSB production crushes the parenchyma cells and the UF resin covers all cells and hinders water penetration. Thus it is obvious that higher density OBSBs with lower porosity reveal lower WA% values (Figure 3).

The thickness swelling (TS) and the volumetric swelling coefficient (S) of the OBSB were also assessed (Table 3). The TS data are at the three density levels 11.3, 10.2, and 7.9% (T-OBSB), respectively. The observed differences are significant ($P > 0.05$), thus the TS decrement as a function of density is relevant. Kojima and Suzuki (2011) found similar data for panels after accelerated aging. Nugroho and Ando (2001) discussed the properties of LLB and presented TS data between 2.2% and 5.2% for densities between 0.6 and

Brought to you by | National Chung Hsing University
Authenticated
Download Date | 6/16/18 5:13 AM

Table 3: Thickness swelling coefficient (TS%) and volumetric swelling coefficient (S%) of OBSB boards made of *P. pubescens*.

Samples	TS (%)	S (%)
T-OBSB$_{0.8}$	11.35^{b} (0.53)	18.66^{c} (1.33)
T-OBSB$_{0.9}$	10.23^{a,b} (0.84)	15.6^{b} (1.66)
T-OBSB$_{1.0}$	7.93^{a} (1.23)	11.24^{a} (1.82)
C-OBSB$_{0.8}$	17.32^{c} (0.86)	25.64^{e} (0.30)
C-OBSB$_{0.9}$	16.17^{c} (1.58)	22.68^{d} (0.76)
C-OBSB$_{1.0}$	15.41^{c} (1.16)	19.12^{c} (1.39)

Numbers followed by different letters (a–e) are statistically different at the probability level of $p < 0.05$ accoring to Tukey's test and ANOVA.

0.9 g cm^{-3}. Furthermore, the swelling coefficient (S%) values of C-OBSB$_{0.8,\ 0.9,\ 1.0}$ were 25.6, 22.7, and 19.1%, respectively. The corresponding data for T-OBSB are 18.7, 15.6, and 11.2%, respectively. The differences between the groups ($P > 0.05$) are significant. The positive influence of extractives on the dimensional stability of lignocellulosic was pointed out by Umezawa (2001). The swelling coefficient (S%) values of C-OBSB are higher than those of T-OBSB. Perhaps, the higher alcohol-benzene extractive content of moso bamboo from China is responsible for this observation (Chung and Wang 2017).The S% is higher than the TS% for both groups. S% is the sum of the dimensional change in length, width and thickness direction and it is more susceptible to density changes than TS%. In summary, there are inverse relationships between WA%, TS% and S% and density.

Conclusions

The $V_{u(//)}$, MOE, MOR and IB values of C-OBSB and T-OBSB show positive relationships with density. Due to chemical composition differences of moso bamboo from Taiwan and China, the mechanical properties of C-OBSB are significantly lower than those of T-OBSB. Among all specimens, T-OBSB$_{0.9}$ showed the best MOR value (172.9 MPa) among all samples. At elevated densities, the profile density at the surfaces was pronouncedly higher than in the center of the boards, but the density distribution of C-OBSB is relatively homogenous. The IB value of T-OBSB was significantly higher than that of C-OBSB. In general, the T-OBSB is superior to C-OBSB. The SB data of all OBSBs are similar if the densities are around 1.0 g cm^{-3}. At the same density level, the WAP of C-OBSB is higher than that T-OBSB. The WAP, TS and S data are inversely proportional to density. The reasons for the chemical and other differences from moso bamboo from China and Taiwan, assuming their genetic identity, are still waiting to be explained.

Acknowledgment: This study was financially supported by a Grant (106-A03-5) from the Experimental Forest, College of Bioresource and Agriculture, National Taiwan University, Taiwan.

References

American Society for Testing and Methods. (1999) ASTM D1037, Evaluating properties of wood-based fiber and particle panel materials.

Chung, M.J., Wang, S.Y. (2017) Effects of peeling and steam-heating treatment on basic properties of two types of bamboo culms (*Phyllostachys makinoi* and *Phyllostachys pubescens*). J. Wood Sci. 1–10.

Hon, N.S. Wood and cellulosic chemistry. Marcel Dekker, Inc., New York, 2001.

Huang, P., Pickering, S.G., Chang, W.-S., Ansell, M.P., Chew, J.Y.M., Shea, A. (2017) Thermal diffusivity measurement of *Phyllostachys edulis* (Moso bamboo) by the flash method. Holzforschung 71:349–354.

Khalil, H.P.S.A., Bhata, I.U.H., Jawaid, M., Zaidon, A., Hermawan, D., Hadi, Y.S. (2012) Bamboo fibre reinforced biocomposites: a review. Mater. Des. 42:353–368.

Kojima, Y., Suzuki S. (2011) Evaluating the durability of wood-based panels using internal bond strength results from accelerated aging treatments. J. Wood Sci. 57:7–13.

Lee, A.W.C., Bai, X., Peralta, P.N. (1996) Physical and mechanical properties of strandboard made from moso bamboo. For. Prod. J. 46:84–88.

Lee, A.W.C., Bai, X., Bangi, A.P. (1998) Selected properties of laboratory-made laminated bamboolumber. Holzforschung 52:207–210.

Lee, A.W.C., Liu, Y. (2003) Selected physical properties of commercial bamboo flooring. For. Prod. J. 53:23–26.

Lee, C.H., Chung, M.J., Lin, C.H., Yang, T.H. (2012) Effects of layered structure on the physical and mechanical properties of laminated moso bamboo (*Phyllosachys edulis*) flooring. Constr. Build. Mater. 28:31–35.

Li, Y., Yin, L., Huang, C., Meng, Y., Fu, F., Wang, S., Wu, Q. (2015) Quasi-static and dynamic nanoindentation to determine the influence of thermal treatment on the mechanical properties of bamboo cell walls. Holzforschung 69:909–914.

Li, Y., Huang, C., Wang, L., Wang, S., Wang, X. (2017) The effects of thermal treatment on the nanomechanical behavior of bamboo (*Phyllostachys pubescens* Mazel ex H. de Lehaie) cell walls observed by nanoindentation, XRD, and wet chemistry. Holzforschung 71:129–135.

Lin, H.C., Huang, J.C. (2001) Apply fade effective image processing analysis technique to evaluate internal bond strength of particle board (in Chinese language). Taiwan J. For. Sci. 23:77–86.

Lin, C.J., Tsai, M.J., Wang S.Y. (2006) Nondestructive evaluation techniques for assessing dynamic modulus of elasticity of moso bamboo (*Phyllosachys edulis*) lamina. J. Wood Sci. 52:342–347.

Liu, H., Jiang, Z., Fei, B., Hse, C., Sun, Z. (2015) Tensile behaviour and fracture mechanism of moso bamboo (*Phyllostachys pubescens*). Holzforschung 69:47–52.

Liu, H., Wang, X., Zhang, X., Sun, Z., Jiang, Z. (2016) In situ detection of the fracture behaviour of moso bamboo (*Phyllostachys pubescens*) by scanning electron microscopy. Holzforschung 70:1183–1190.

Brought to you by | National Chung Hsing University
Authenticated
Download Date | 6/16/18 5:13 AM

Mishiro, A. (1996) Effect of density on ultrasonic velocity in wood. Mokuzai Gakkaishi 42:887–894.

Nugroho, N., Ando, N. (2001) Development of structural composite products made from bamboo II: fundamental properties of laminated bamboo lumber. J. Wood Sci. 47:237–242.

Obataya, E., Kitin, P., Yamauchi, H. (2007) Bending characteristics of bamboo (*Phyllosachys pubescens*) with respect to its fiber-foam composite structure. Wood Sci. Technol. 41:385–400.

Okubo, K., Fujii, T., Yamamoto, Y. (2004) Development of bamboo-based polymer composites and their mechanical properties. Compos. Pt. A-Appl. Sci. Manuf. 35:377–383.

Oliveira, F.G.R., Campos, J.A.O., Sales, A. (2002) Ultrasonic measurements in Brazilian hardwood. Mater. Res. 5:51–55.

Qu, C., Kishimoto, T., Ogita, S., Hamada, M., Nakajima, N. (2012) Dissolution and acetylation of ball-milled birch (*Betula platyphylla*) and bamboo (*Phyllostachys nigra*) in the ionic liquid [Bmim]Cl for HSQC NMR analysis. Holzforschung 66:607–614.

Ross, R.J. (2015) Nondestructive Evaluation of Wood: Second Edition. USDA Forest Service, Forest Products Laboratory, General Technical Report, FPL-GTR-238. 176 p.

Sharma, B., Gatóo, A., Bock, M., Ramage, M. (2015a) Engineered bamboo for structural applications. Constr. Build. Mater. 81:66–73.

Sharma, B., Gatóo, A., Ramage, M.H. (2015b) Effect of processing methods on the mechanical properties of engineered bamboo. Constr. Build. Mater. 83:95–101.

Sulastiningsih, I.M., Nurwati. (2009) Physical and mechanical properties of laminated bamboo board. J. Trop. For. Sci. 21:246–251.

Tabarsa, T., Chui, Y.H. (1997) Effects of hot-pressing on properties of white spruce. For. Prod. J. 47:71–76.

Umezawa, T. (2001) Chemistry of extractives. In: Wood and Cellulosic Chemistry. Eds. Hon, D.N.S. Shiraishi, N. Marcell Dekker, Inc., New York. pp. 213–241.

Verma, C.S., Chariar, V.M. (2012) Development of layered laminate bamboo composite and their mechanical properties (in Chinese language). Compos. Pt. B-Eng. 43:1063–1069.

Wang, J.X. (1989) Bamboo scrimber – novel technology, novel product. China Wood Ind. 3:54–55.

Wang, S.Y., Chen, J.H., Tsai, M.J., Lin, C.J., Yang, T.H. (2008) Grading of softwood lumber using non-destructive techniques. J. Mater. Process. Technol. 208:149–158.

Wang, H., Zhang, X., Jiang, Z., Yu, Z., Yu, Y. (2016) Isolating nanocellulose fibrills from bamboo parenchymal cells with high intensity ultrasonication. Holzforschung 70:401–409.

Wen, J.L., Sun, S.-L., Xue, B.-L., Sun, R.-C. (2013) Quantitative structural characterization of the lignins from the stem and pith of bamboo (*Phyllostachys pubescens*). Holzforschung 67:613–627.

Winistorfer, P.M., Xli, W., Wimmer, R. (1995) Application of a drill resistance technique for density profile measurement in wood composite panels. For. Prod. J. 45:50–53.

Yu, W.J., Yu, Y.L. (2013) Development and prospect of wood and bamboo scrimber industry in China (in Chinese language). China Wood Ind. 27:5–8.

Yu, Y., Zhu, R., Wu, B., Hu, Y., Yu, W. (2015) Fabrication, material properties, and application of bamboo scrimber. Wood Sci. Technol. 49:83–98.

Brought to you by | National Chung Hsing University
Authenticated
Download Date | 6/16/18 5:13 AM